

BEARING FAILURE MODE AND STIFFNESS ANALYSIS OF L-SHAPED PARTS CONNECTED BY BEECH AND SELF-TAPPING SCREW COMPOSITE DOWELSXUDONG ZHU^{1,2}¹YANGZHOU POLYTECHNIC INSTITUTE²YANGZHOU UNIVERSITY

CHINA

YINGYING XUE, XUEWEN ZHANG, PENGFEI QI, QIAN LAN, JIE SHEN, LIANG QIAN

YANGZHOU POLYTECHNIC INSTITUTE

CHINA

SHENGCAI LI

YANGZHOU UNIVERSITY

CHINA

(RECEIVED JUNE 2022)

ABSTRACT

This study examined the performance of beech and self-tapping screw composite dowel applied to non-extruded L-shaped member joints and carries out theoretical calculation and analysis of stiffness. The test results indicated that eleven specimens showed three failure modes. It was found that the composite dowel had different degrees of bending phenomenon. The failure modes were also proved by the finite element analysis. Since the spruce-pine-fir was in the middle of the L-shaped specimen set in this test, it can rotate around the geometric center composed of four composite dowels. The correction formula of the elastic rotational stiffness K of the joint

can be presented by
$$K = \left(\frac{0.03\rho^{1.5}d}{1.6} \right) \sum_{i=1}^n r_i^2.$$

KEYWORDS: Beech and self-tapping screw composite dowel, L-shaped component, bearing failure mode, stiffness analysis.

INTRODUCTION

Self-tapping screws and dowels are common connection methods for wood components. However, the self-tapping screw connection node will be loose during the application, and the stiffness is insufficient during the load-bearing process. On the one hand, the compression

friction bearing capacity and rigidity of the joint are improved by matching the metal or plastic expansion tube, as shown in Fig. 1. However, in the case of forcibly screwing in or heavy knocking conditions, it leads to cracking of the wood and even cause the cracking of the metal expansion tube. On the other hand, during the process of screwing in the plastic expansion tube, due to the large aperture, it easily deformed the plastic expansion tube by moving up and squeezing patterns, which resulted in the lower part of the self-tapping screw failing to cover the plastic expansion tube. For wood dowel joints, the length of wood dowel within 50 mm is usually used for joints that cannot meet the application requirements of beam-column section of wood structure with 100 mm or even 400 mm. If a long wooden dowel is used to tap into the beam-column connection, the wooden dowel is easily broken during the knocking process. The method is used to reinforce the wood dowel joint, as shown in Fig. 1. The function of adding metal nails at the bottom is that during the knock-in process, the metal nails are embedded in the wood dowel to cause the expansion of the wood dowel, which increases the extrusion friction. However, it causes the cracking of the local wood dowel. Meanwhile, when the hardness of the wood dowel is higher than that of the base material, the metal nail will sink into the base material and cannot achieve the effect of the fastening function. Adding adhesive in the hole wall of the substrate can easily cause uneven distribution of the glue or overflow the surface to form glue spots and poor adhesion.



Fig. 1: The disadvantages of the joints connected by wood dowels and self-tapping screws.

The wood dowel welding technology is a method of fast-rotating friction, which makes the wood dowel and the surface of the wood pre-drilled hole generate much heat, which causes the three major components of cellulose hemicellulose and lignin in the wood to be pyrolyzed and melted. A black molten substance forms a cohesive interface after cooling and solidifying (Zhou et al. 2014, Luo et al. 2017). Many researchers have analyzed the mechanical properties of wood-dowel welded joints, especially the pull-out resistance of wood dowels. On the one hand, Auchet et al. (2010 and Belleville et al. (2013) analyzed the effects of the rotation speed and insertion speed of maple and birch on the pull-out resistance of the joint. The optimal insertion speed of maple and birch was $25 \text{ mm}\cdot\text{s}^{-1}$ and $16.7 \text{ mm}\cdot\text{s}^{-1}$, respectively.

Moreover, it was concluded that the optimum speed for beech wood dowels was 1500 rpm in several researches (Chedeville et al. 2005, Pizzi et al. 2006, Leban et al. 2008). In our previous study, birch wood dowels were welded to larch substrates, the optimal rotational speed was 2400 rpm (Rodriguez et al. 2010), and the insertion speed was $10 \text{ mm}\cdot\text{s}^{-1}$ (Zhu et al. 2019). On the other hand, Belleville found that the pull-out resistance of the maple dowel welded joint was higher than that of the birch dowel welded joint under the same conditions. It was found that the

black molten material at the welding interface mainly comes from the wooden dowel (Belleville et al. 2013a). Similar conclusions were found that the optimal speed of beech dowel was 1500 rpm, and the pull-out resistance of the welded interface was 30% higher than that of birch dowel welded joints (Xue et al. 2022). In terms of the ratio of dowel diameter to pre-drilled diameter, it was found that when the ratio of dowel diameter to pre-drilled diameter was about 1.25, the pull-out resistance of the welded joint of the dowel was the largest value (Bocquet et al. 2007, Kanazawa et al. 2005, Zhu et al. 2019).

Meanwhile, the dry wood dowel is used for welding combined with dry shrinkage and swelling of the wood. After the welding process, the joint absorbs water vapor in the air. As the moisture content increases, the wood dowel also expands in volume, which further increases the wood dowel and squeezes friction between the walls of pre-drilled holes. Therefore, the pull-out resistance of welded joints increases. Furthermore, dry wood dowels can improve the pull-out resistance of welded joints (Kanazawa et al. 2005, Segovia et al. 2009, Zhu et al. 2019). In the study of other pretreated method, the wood dowel pretreated with citric acid could improve the pullout resistance (Amirou et al. 2017).

Wood dowel welding was used to prepare multi-layered beams of glulam and establish a structural stress model for the application of wood dowel welding instead of adhesives (Loinsigh et al. 2012, Belleville et al. 2013b, Girardon et al. 2014). Moreover, Bocquet et al. (2007) investigated the vertical and horizontal lap joints of wood laminates to form floor slabs and used wood dowel welding to connect the lap joints, which had better stiffness than no joints. During the load-bearing process of multi-layer beams and floor slabs, the dowels were subjected to shear and uplift forces between layers (Belleville et al. 2011). The bonding strength of the welding interface was required relatively high. However, the interface strength of the wood-dowel welding cannot reach the structural level. So, the overall component bearing capacity and stiffness are not high (Bocquet et al. 2007, Girardon et al. 2014).

Furthermore, Satoshi used a 10 mm diameter dowel as a shear connector to fix the frame shear wall. Compared with the 2.85 mm diameter nail-connected frame shear wall under the same test conditions, it has higher lateral strength and stiffness. However, the ductility and energy consumption are insufficient, and it is easy to break and damage (Satoshi et al. 2017). Jia et al. (2021) found that the allowable deformation of the wood-dowel welded joint was negligible during the double-shear bearing test process, which was easily broken. It was shown that the ductility and energy consumption of the wood dowel was poor. On the other hand, the bamboo dowel was used to connect wood by rotation. The pullout resistance of bamboo dowel was higher than the wood dowel on the same diameter, but the bamboo dowel was also broken easily (Li et al. 2021, Yang et al. 2022).

There is a need to solve the problem of improving wood dowel welding node toughness, ductility, and energy dissipation, which postpones the fracture process of the wood dowel. The steel pipe and PVC casing are successively set on the outer side of the metal bolt. The adhesive is applied at the gap to enhance stiffness and reduce slip, which refers to the research study of He et al. (2013). Combined with the mechanical characteristics of the wood dowel and self-tapping screw in the load-bearing process, Xue et al. (2022) designed a new type of beech and self-tapping screw composite dowel. Moreover, the bearing capacity of the

composite dowel connection with a single shear specimen is analyzed. Based on the above research, this paper further studies the performance of composite dowel applied to non-extruded L-shaped member joints and carries out theoretical calculation and analysis of stiffness (Mougel et al. 2011).

MATERIAL AND METHODS

Materials

Spruce-pine-fir (SPF) timber, with a section of 38×89 mm, a material grade of Class II, an average density of $495 \text{ kg}\cdot\text{m}^{-3}$, and a moisture content of 9.7%, which is provided by Suzhou Crownhomes Co., Ltd. The self-tapping screws 6 x 120 mm with galvanized surface were provided by Shanghai Moregood Co., Ltd (Tab. 1).

Tab. 1: Technical specifications of self-tapping screws.

Nominal diameter	Thread bottom diameter	Polished rod diameter	Head diameter
6 mm	4 mm	4.3 mm	12 mm
Bending yield strength	Pull-out strength	Tensile strength	Tensile load
1000 MPa	14.4 MPa	1100 MPa	13.8 kN

The diameter of the beech wood dowel is 12 mm, and the length is 100 mm. The average density is $703 \text{ kg}\cdot\text{m}^{-3}$, and the moisture content is 2%, which is provided by Suzhou Crownhomes Co., Ltd. The specific steps of beech wood dowel embedded with self-tapping screws to form a composite dowel (Fig. 2) are as follows: (1) A 3.5 mm pre-drilled hole is opened at the center of the beech dowel section, which penetrates the entire beech dowel. (2) The self-tapping screw is screwed into the pre-drilled hole of the beech dowel for 95 mm, with the head exposed for 25 mm.

Methods

The components used in the test include a cross-cut saw, computer-controlled electronic universal test machine (Jinan Assay Group Co., Ltd., maximum force: 100 kN), claw hammer, electric hand drill, and bench drill. The schematic diagram of the specimen without extruded L-shaped member is shown in Fig. 3a. The steps for inserting the composite dowel into the specimen are as follows: (1) A pre-drilled hole with a diameter of 10 mm and a depth of 100 mm is opened, and the specimen needs to be connected. (2) A clamping block is used to fix the exposed 25 mm self-tapping screw in the bench drill, as shown in Fig. 2. It can drive the composite dowel into the test piece at a speed of 1500 rpm and an insertion speed of $10 \text{ mm}\cdot\text{s}^{-1}$; (3) The clamping block is removed, and then it uses a pistol drill to completely screw the exposed 25 mm of the self-tapping screw into the beech dowel.

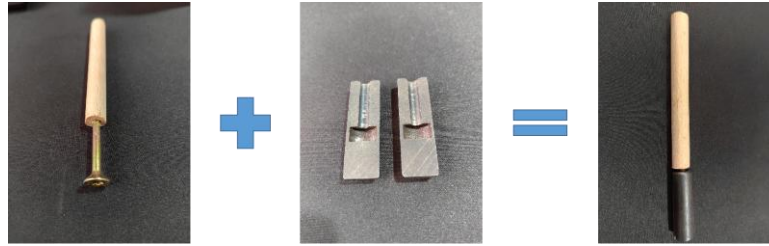


Fig. 2: The composite dowel packed by the clamping block.

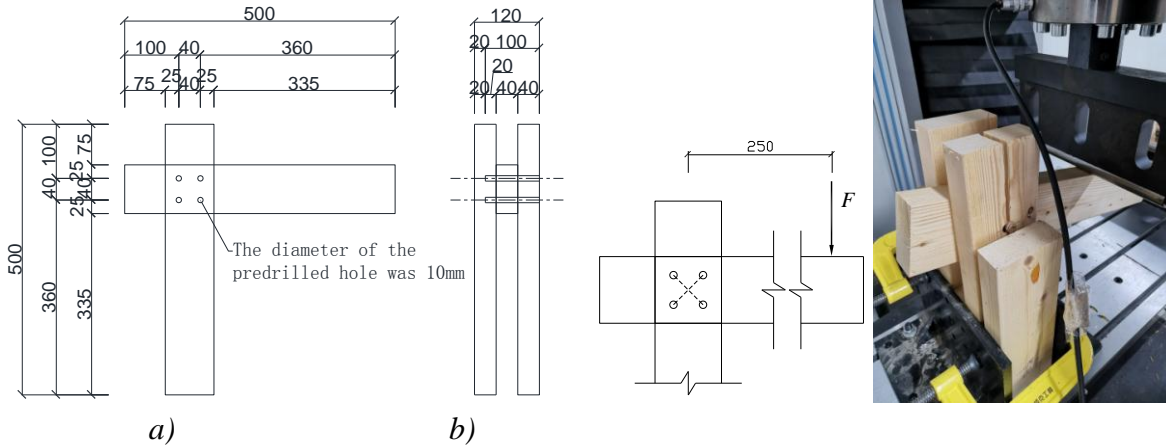


Fig. 3: Test specimen: a) The sketch map of the specimen, b) The loading method.

The number of specimens is eleven (No.1- No.11), and the loading method is shown in Fig. 3b. The loading point is 250 mm away from the geometric center composed of four composite dowels. All the specimens were conditioned at 20°C and 60% RH for 7 days before the tests were conducted.

RESULTS AND DISCUSSION

Failure mode of specimens

The force versus displacement curves of the eleven specimen nodes is shown in Fig. 4. The average maximum shear force is 3.95 kN (the standard deviation was 0.32), and the average stiffness is 11.92 kN·mrad⁻¹ (the standard deviation was 3.14).

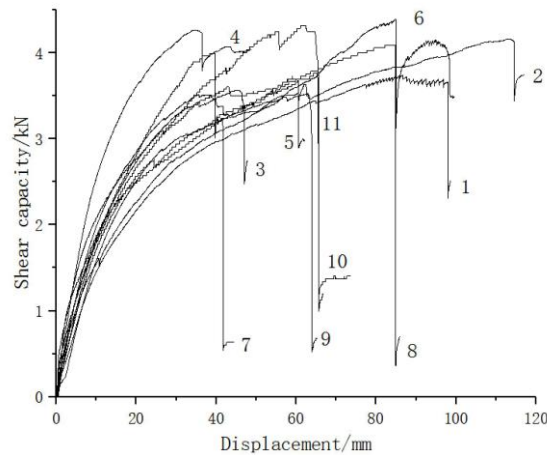


Fig. 4: The load-displacement curve of the six specimens.

As shown in Fig. 5, the eleven specimens in this test showed three failure modes. One of the SPF grades on both sides of the No. 3, No. 4, and No. 7 specimens suffered splitting failure (Fig. 5a). The middle SPF wood of specimens No. 1, No. 2, No. 6, and No. 8 were split. (Fig. 5b). Moreover, the two sides and middle SPF wood of specimens No. 5, No. 9, No. 10, and No. 11 were split to varying degrees (Fig. 5c).

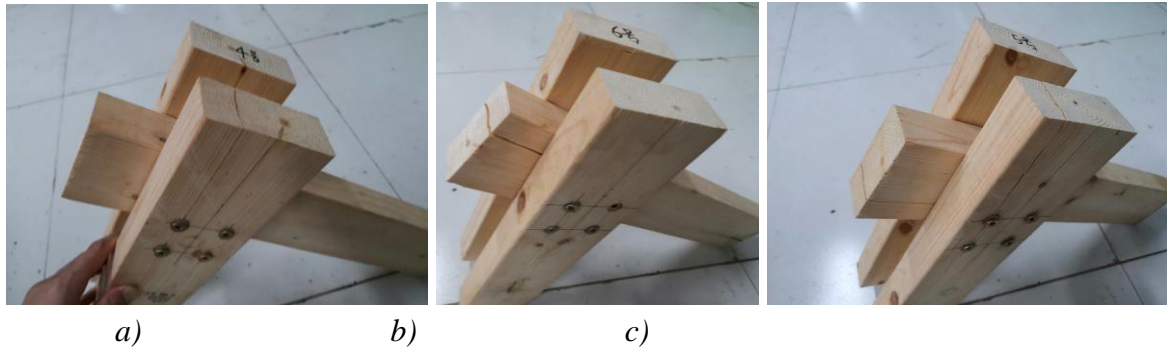


Fig. 5: Failure modes: a) Outer side splitting, b) Splitting in the middle specimen, c) Outer sides and middle specimen splitting.



Fig. 6: The failure mode of composites dowel.

It was found that the composite dowel joints had different degrees of bending phenomenon. The surface of the beech wood dowel had a splitting phenomenon, and the hole wall was squeezed and deformed (Fig. 6).

All the specimens had good coincidence before the displacement reached 10 mm. The bearing capacity of the No. 4 specimen increased rapidly. When the displacement of the No. 3, No. 4, and No. 7 specimens was about 40 mm, one of the SPF specifications on both sides occurred as splitting. The SPFs on both sides were clamped and fixed during the test. The energy cannot be dissipated by rotation during the bearing process, and the bearing force can only be concentrated on the hole wall. If the cracking limit was reached, the damage occurred. No. 1, No. 2, No. 6, and No. 8 specimens had good ductility, and the displacement deformation reached more than 80 mm. The intermediate SPF specification can be rotated during the loading process, which reduces the influence of the loading process on the hole wall. In the case of no splitting of the side SPF material, the middle SPF specification material eventually splits at the connection cavity due to the large displacement and deformation. Specimen No. 5, No. 9, No. 10, and No. 11 showed special failure mode with split failures on both sides and in the middle, which resulted in a smaller final bearing capacity and smaller ultimate displacement.

Finite element analysis

There are nine parameters for the orthotropy of wood, including elastic moduli E_1 , E_2 , and E_3 in three directions, three shear moduli G_{12} , G_{13} , G_{23} , and three Poisson's ratios ν_{12} , ν_{13} , ν_{23} . It can be seen from the material property that the elastic modulus along the grain of the SPF material is 5809 MPa (Du et al. 2022). The remaining elastic and shear modulus can be converted according to the proportional formula, as shown in Tab. 2. The subscripts 1, 2, and 3 represent the longitudinal, radial, and chord directions of the wood, respectively. For the Poisson's ratio of SPF specifications, it is recommended to take $\nu_{12} = 0.3$, $\nu_{13} = 0.42$, and $\nu_{23} = 0.30$. The parameters of the beech dowel obtained by the same method are shown in Tab. 2.

Tab. 2: Modeling parameters of SPF lumber and beech dowels.

Parameters	E_1 (MPa)	E_2 (MPa)	E_3 (MPa)	ν_{12}	ν_{13}	ν_{23}	G_{12} (MPa)	G_{13} (MPa)	G_{23} (MPa)
SPF specification material	5809	581	290	0.3	0.42	0.3	349	436	105
Wood dowel	12567	1374	579	0.450	0.554	0.841	899	595	195

The self-tapping screw is simplified as an ideal elastic-plastic body, f_y is the yield strength of the steel with 550 MPa. The value of strain ϵ_0 is 0.29%, and the Poisson's ratio is 0.3.

Figs. 7 and 8 show the deformation cloud diagrams of the two sides and the middle SPF timber, beech dowels, and self-tapping screws.

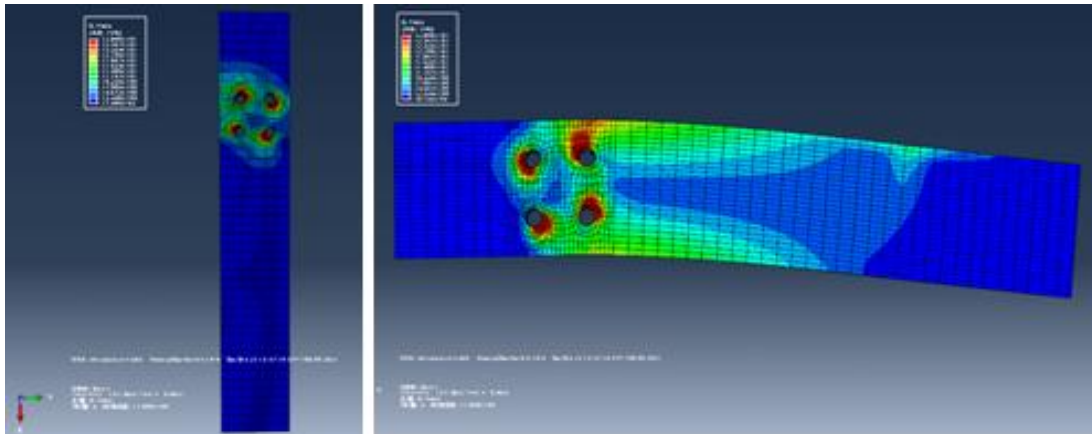


Fig. 7: a) Deformation cloud map of SPF specifications on both sides, b) Deformation cloud map of intermediate SPF material.

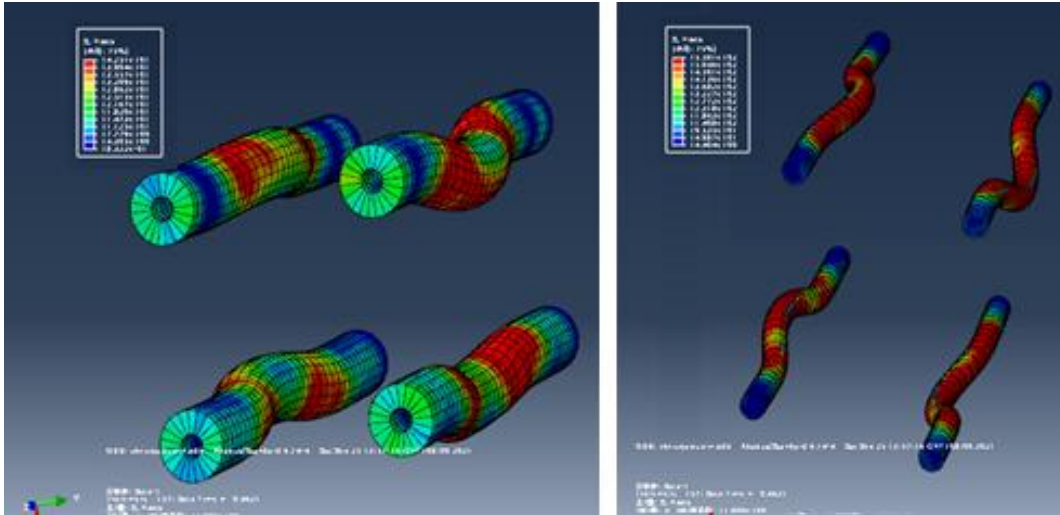


Fig. 8: a) Cloud map of beech dowel deformation, b) Deformation cloud diagram of self-tapping screw.

Due to the clamping constraint of the test fixture, the vertical member did not have obvious deformation in the test and simulation. The transverse member was loaded on one side, and the final deformation was mainly rotated around the geometric center of the connector. The remaining failure of the connecting hole wall of the substrate also accords with the test characteristics In Fig. 8a. It can be seen that the beech dowel is less deformed as one of the components of the composite dowel. As shown in Fig. 8b, the self-tapping screw embedded in the beech dowel had a large deformation. On the one hand, the self-tapping screw has better toughness, which can withstand large loads and deformations. On the other hand, the self-tapping screw can be embedded in the beech dowel twice to increase the amount of deformation.

Nodal stiffness analysis

According to Eurocode 5, the elastic rotational stiffness of the node can be calculated by Eq. 1:

$$K = \left(\frac{K_{ser}}{1 + K_{def}} \right) \sum_{i=1}^n r_i^2 \quad (1)$$

where: K_{ser} is the slip modulus, calculated regarding Table 7.1 in Eurocode 5; K_{def} is the water content parameter, with reference to Table 3.2 in Eurocode 5, with a value of 0.6; r_i is the straight-line distance from the first compound dowel to the rotational geometric center.

Li et al. (2021) have studied the shear force of joints at different positions, which presents different angles to the direction along the grain under the action of bending moment. However, Eurocode 5 does not consider the effect of different angles on the shear-slip modulus of the connector. In the study, the calculation formula of the slip modulus K_{ser} of each shear surface of each fastener based on the formula in Table 7.1 in Eurocode 5, which was revised as:

$$K_{ser} = 2\rho^{u_1} d / \mu_2 \quad (2)$$

where: ρ is the density of the SPF specification material of 495 kg m^{-3} , and d is the diameter of the composite dowel 12 mm.

Compared with the formula in the original Eurocode 5, the correction coefficient 2 is added. The parameters 1.5 and 23 in Eurocode 5 are defined as the regression coefficients u_1 and μ_2 , respectively. Based on the experimental test results, Li revised the regression coefficients to 1.5 and 28. In this paper, there are double effects of interference fit and welding glue between the composite dowel and the hole wall of the connecting member. The correction coefficient 2 is added, and the regression coefficient is corrected to 1.5 and 133, respectively. The joint type is double Scissor joints so that the slip modulus K_{ser} of each composite dowel can be calculated by the Eq. 3:

$$K_{ser} = 4\rho^{1.5}d / 133 = 0.03\rho^{1.5}d \quad (3)$$

Bringing Eq. 3 into Eq. 1, the correction formula of the elastic rotational stiffness K of the node can be obtained:

$$K = \left(\frac{0.03\rho^{1.5}d}{1.6} \right) \sum_{i=1}^n r_i^2 \quad (4)$$

Since the SPF material is in the middle of the L-shaped member set in this test, it can rotate around the geometric center composed of four composite dowels. All of them here are 34.65 mm. The theoretical value of the elastic rotational stiffness of the joints in this study is $11.93 \text{ kN}\cdot\text{m}\cdot\text{rad}^{-1}$ by Eq. 4. Tab. 3 illustrates the comparison results between the theoretical and experimental values of all the joints of the specimens, which are all between 0.70 and 1.72. In the study of Li et al. (2021), the same formula was used to calculate the elastic stiffness of bolted connections in the glulam, the ratios of experimental and theoretical values were between 0.84 and 1.54. In this study, the anisotropy properties and defects of SPF and beech dowels influence the test values. The minimum value and Maximum value of the elastic stiffness of the specimens showed big difference between $6.94 \text{ kN}\cdot\text{m}\cdot\text{rad}^{-1}$, and $17.12 \text{ kN}\cdot\text{m}\cdot\text{rad}^{-1}$.

Tab. 3: Comparison results of experimental and theoretical values of elastic stiffness of joints.

Specimen label	1	2	3	4	5	6	7	8	9	10	11
Test value ($\text{kN}\cdot\text{m}\cdot\text{rad}^{-1}$)	7.22	9.89	10.94	17.12	12.39	6.94	13.70	11.51	15.69	12.57	13.10
Theoretical value/ Experimental value	1.65	1.21	1.09	0.70	0.96	1.72	0.87	1.04	0.76	0.95	0.91

CONCLUSIONS

(1) The six specimens showed three failure modes. One of the SPF grades on both sides of the No. 3, No. 4, and No. 7 specimens suffered splitting failure. The middle SPF wood of specimen No. 1, No. 2, No. 6, and No. 8 were split. Moreover, the two sides and middle SPF wood of specimens No. 5, No. 9, No. 10 and No. 11 were split to varying degrees. (2) It was

found that the composite dowel had different degrees of bending phenomenon. The failure modes were also proved by the finite element analysis. (3) Since the Spruce-pine-fir was in the middle of the L-shaped specimen set in this test, it can rotate around the geometric center composed of four composite dowels. The correction formula of the elastic rotational stiffness K

of the joint can be presented by
$$K = \left(\frac{0.03\rho^{1.5}d}{1.6} \right) \sum_{i=1}^n r_i^2 .$$

ACKNOWLEDGMENTS

The authors are grateful for the support of the National Natural Science Foundation of China (Grant No. 31901252), the Jiangsu Planned Projects for Postdoctoral Research Funds (Grant No. 2020Z075), the Science and Technology Program of Jiangsu Housing and Construction Department (No. 2020ZD39, 2021ZD22), Qing Lan Project of Jiangsu, the Yangzhou Science and Technology Project (Grant No. YZ2022110), and the Natural Science Foundation of the High Education Institutions of Jiangsu Province (Grant No. 22KJA220003). The authors thank TopEdit (www.topeditsci.com) for its linguistic assistance during the preparation of this manuscript.

REFERENCES

1. Amirou, S., Pizzi, A., Delmotte, L., 2017: Citric acid as waterproofing additive in butt joints linear wood welding. *European Journal of Wood and Wood Products* 75(4): 651-654.
2. Auchet, S., Segovia, C., Mansouri, H.R., 2010: Accelerating vs constant rate of insertion in wood dowel welding. *Journal of Adhesion Science and Technology* 24(7): 1319-1328.
3. Belleville, B., Segovia, C., Pizzi, A., Stevanovic, T., Cloutier, A., 2011: Wood blockboards fabricated by rotational dowel welding. *Journal of Adhesion Science and Technology* 25: 2745-2753.
4. Belleville, B., Stevanovic, T., Pizzi, A., Cloutier, A., Blanchet, P., 2013a: Determination of optimal wood welding parameters for two North American hardwood species. *Journal of Adhesion Science and Technology* 27(5-6): 566- 576.
5. Belleville, B., Stevanovic, T., Cloutier, A., Pizzi, A., Salenikovich, A., Blanchet, P., 2013b: Production and properties of wood-welded panels made from two Canadian hardwoods. *Wood Science and Technology* 47: 1005-1018.
6. Bocquet, J. F., Pizzi, A., Resch, L., 2007: Full-scale industrial wood floor assembly and structures by welded-through dowels. *European Journal of Wood and Wood Products* 65(2): 149-155.
7. Chedeville, C. G., Pizzi, A., Thomas, A., Leban, J.M., Bocquet, J.F., Despres, A., Mansouri, H., 2005: Parameter interactions in two-block welding and the wood nail concept in wood dowel welding. *Journal of Adhesion Science and Technology* 19(13-14): 1157-1174.

8. Du, Y.Y., Zhang, S.J., Zhu, X.D., Zhang, W.J., 2022: Research on axial compression performance of 4-leg standard lumber lattice columns. *Journal of Forestry Engineering* 7(03): 158-165.
9. Girardon, S., Barthram, C., Resch, L., Bocquet, J.F., Triboulot, P., 2014: Determination of shearing stiffness parameters to design multi-layer spruce beams using welding-through wood dowels. *European Journal of Wood and Wood Products* 72(6): 721-733.
10. He, M.J., Ni, S.N., Ma, R.L., Bai, X., 2013: Loading tests of prestressed tube bolted joint with slotted-in steel plate. *Journal of Tongji University (Natural Science)* 41(9): 1353-1358.
11. Jia, H.R., Wang, N., Meng, X.M., Gao, Y., Zhu, X.D., 2021: Effects of inclined degree on shear performance of wood-dowel rotation welding joints. *Guangxi Forestry Science* 50(3): 252-258.
12. Kanazawa, F., Pizzi, A., Properzi, M., Delmotte, L., Pichelin, F., 2005: Parameters influencing wood-dowel welding by high-speed rotation. *Journal of Adhesion Science and Technology* 19(12): 1025-1038.
13. Leban, J.M., Mansouri, H.R., Omrani, P., Pizzi, A., 2008: Dependence of dowel welding on rotation rate. *European Journal of Wood and Wood Products* 66(3): 241-242.
14. Li, S.X., Zhang, H.Y., Cheng, L.S., Ju, Z.H., Lu, X.N., 2021: Bonding properties of bamboo dowel (nail) welded to wood with high-speed rotation. *Journal of Northwest Forestry University* 36(4): 225-232.
15. Li, Z., Luo, J., He, M.J., Yu, X.S., Liang, F., Shu, Z., Sun, Y.L., 2021: Analytical investigation into the rotation behavior of glulam bolted connections with slotted-in steel plates under coupled bending moment and shear force. *China Civil Engineering Journal* 54(3): 98-108.
16. Loinsigh, C.O., Oudjene, M., Shotton, E., Pizzi, A., Fanning, P., 2012: Mechanical behaviour and 3D stress analysis of multi-layered wooden beams made with welded-through wood dowels. *Composite Structures* 94(2): 313-321.
17. Luo, X.Y., Zhu, X.D., Zhang, J.R., Gao, Y., 2017: Theoretical research and technical progress of wood welding. *Journal of Northwest Forestry University* 32(6): 270-275.
18. Mougel, E., Segovia, C., Pizzi, A., Thomas, A., 2011: Shrink-fitting and dowel welding in mortise and tenon structural wood joints. *Journal of Adhesion Science and Technology* 25: 213-221.
19. Pizzi, A., Despres, A., Mansouri, H.R., Leban, J.M., Rigolet, S., 2006: Wood joints by through-dowel rotation welding: microstructure and ¹³C-NMR and water resistance. *Journal of Adhesion Science and Technology* 20(5): 427-436.
20. Rodriguez, G., Diouf, P., Blanchet, P., Stevanovic, T., 2010: Wood-dowel bonding by high-speed rotation welding - application to two Canadian hardwood species. *Journal of Adhesion Science and Technology* 24: 1423-1436.
21. Satoshi, F., Keita, O., Masaki, N., Mariko, Y., Yasutoshi, S., 2017: Shear properties of metal-free wooden load-bearing walls using plywood jointed with a combination of adhesive tape and wood dowels. *European Journal of Wood and Wood Products* 75(3): 429-437.
22. Segovia, C., Pizzi, A., 2009: Performance of dowel-welded wood furniture linear joints. *Journal of Adhesion Science and Technology* 23: 1293-1301.

23. Xue, Y.Y., Zhu, X.D., Zhang, X.W., Qi, P.F., Li, J.J., Zhu, L.H.R., Yao, L.H., 2022: Single shear performance of components connected by beech-self-tapping-screw composite dowels. *Chinese Journal of Wood Science and Technology* 36(1): 68-74.
24. Yang, H.D., Wang, N., Meng, X.M., Zhu, X.D., Gao, Y., 2022: Study on process parameters and mechanism of bamboo dowel rotation welding. *Journal of Beijing Forestry University* 44(2): 141-150.
25. Zhou, X.J., Pizzi, A., Du, G.B., 2014: Research progress of wood welding technology (bonding without adhesive). *China Adhesives* 23(6): 47-53.
26. Zhu, X.D., Xue, Y.Y., Shen, J., Zhang, S.J., 2019: Withdrawal strength of welded dowel joints made of birch and larch wood. *Wood Research* 64(5): 921-934.

XUDONG ZHU^{1,2}

¹YANGZHOU POLYTECHNIC INSTITUTE
COLLEGE OF BUILDING ENGINEERING

NO. 199, HUAYANG WEST ROAD, HANJIANG DISTRICT, YANGZHOU CITY

²YANGZHOU UNIVERSITY

COLLEGE OF BUILDING SCIENCE AND ENGINEERING

NO. 196, HUAYANG WEST ROAD, HANJIANG DISTRICT, YANGZHOU CITY

JAINGSU PROVINCE

CHINA

YINGYING XUE, XUEWEN ZHANG, PENGFEI QI, QIAN LAN, JIE SHEN, LAING QIAN

YANGZHOU POLYTECHNIC INSTITUTE

COLLEGE OF BUILDING ENGINEERING

NO. 199, HUAYANG WEST ROAD, HANJIANG DISTRICT, YANGZHOU CITY,

JAINGSU PROVINCE

CHINA

SHENGCAI LI*

YANGZHOU UNIVERSITY

COLLEGE OF BUILDING SCIENCE AND ENGINEERING

NO. 196, HUAYANG WEST ROAD, HANJIANG DISTRICT, YANGZHOU CITY,

JAINGSU PROVINCE

CHINA

*Corresponding author: li_shcai@126.com